Exciton dissociation, charge transport, and recombination in ultrathin, conjugated polymer-TiO_2 nanocrystal intermixed composites

J. S. Salafsky
Debye Institute, Faculty of Physics and Astronomy, Universiteit Utrecht, P.O. Box 80,000, NL-3508 TA Utrecht, The Netherlands
(Received 5 August 1998)

A detailed study of the optoelectronic processes occurring in ultrathin TiO_2 nanocrystal-conjugated polymer, poly(*p*-phenylene vinylene) (PPV) composites is presented. Composites of ultrathin films (about 100 nm) are studied spectroscopically and as the active medium in photovoltaic devices of the structure (Al/composite/indium tin oxide). By varying the weight ratio of the nanocrystals and using results of photoluminescence efficiency, photocurrent, and photovoltaic measurements and time-resolved microwave conductivity, we are able to construct a well-defined picture of the relevant processes in the composite: including exciton dissociation, charge transport, and recombination. We combine the experimental results with a hopping model for charge transport in a nanocrystal lattice (random walk or biased random walk) to determine the probability of electron collection as a function of distance from a collecting contact in a nanocrystal lattice. The combined results indicate that most photogenerated excitons lead to charge separation at the interface between the polymer and the nanocrystals above 20-wt % TiO_2 nanocrystals, but the electron collection efficiency in photovoltaic devices is limited by fast recombination. The transport model indicates that even for a relatively long recombination time and a well-ordered nanocrystal lattice, most of the collected charge will originate from the first several nanocrystal layers at the electrode rather than from sites throughout the film, due to the recombination process. We also argue that the existence of a photocurrent in these and related devices is not necessarily evidence of charge transport through a network of the nanocrystals (or other component), as the quantum yields can be accounted for by interfacial charge transfer at the contact alone. Quantum yields for collecting charge following direct band-gap excitation of the TiO_2 are more than a factor of 10 larger than for excitation into the polymer, suggesting that either hole transfer to the polymer, or some preceding process, is rate limiting and much slower than the corresponding process following polymer excitation. We also examine the key differences between the mechanisms underlying conjugated polymer:nanocrystal devices and conventional, silicon *pn* devices. [S0163-1829(99)02015-9]

I. INTRODUCTION

Semiconductor nanocrystals lie in the mescoscopic size regime between the bulk and molecular. As such, they are of interest in the study of the transition in electronic and optical properties between the two scales. For instance, the band gap and radiative lifetime of the lowest allowed optical excitation can be tuned with size,[1] and single-electron transport events can be seen as discrete steps in conductance.[2] These properties are unique to an intermediate size regime, belonging to neither the molecular or the bulk. Conjugated polymers, macromolecules, also represent an unusual type of material, behaving like a bulk, amorphous, semiconductor in solid-state form.[3] Typical diffusion lengths of singlet excitons, the main species upon photoexcitation, are in the range of 5–15 nm with radiative and nonradiative decay time scales of 100–1000 ps.[4–7]

Composites of semiconductor nanocrystals with conjugated polymers are also interesting as model systems for photoinduced charge transfer at nanometer-scale interfaces. Previous work has demonstrated that photoinduced charge transfer does occur between a derivative of poly(*p*-phenylene vinylene) (PPV) with CdS and CdSe nanocrystals,[8] and photovoltaic devices have been made using composites of the materials as the active medium.[9] Photovoltaic devices using a blend of two conjugated polymers with different electronegativities have also been developed.[10] In these devices the authors demonstrated that the morphology in the blends is structured on a nanometer length scale, which results in an efficient conversion of excitons to separated charges. In related work, a PPV derivative with C_{60} molecules blended in at high weight fractions forms the active medium of photovoltaic devices with high quantum yields.[10–12] In a previous study, we showed directly, using a microwave conductivity technique, that excitons generated in PPV will dissociate at a TiO_2 nanocrystal interface with electrons transferred to the nanocrystals.[13] We are also able to time resolve the dynamics of the recombination process using the same technique, a complex process which occurs on a time scale of hundreds of nanoseconds to microseconds. This key piece of information provides insight into the dynamical processes underlying conjugated polymer-nanocrystal composites, and allows one to construct a model for charge transport based on the composites in a photovoltaic device.

This paper studies PPV:TiO_2 nanocrystal composites, focusing on the photoinduced electron and hole transfer and recombination processes at the interface between the two components, and the charge transport in the polymer and nanocrystal phases. Photovoltaic devices based on a composite of conjugated polymer with TiO_2 nanocrystals are introduced. By combining photoluminescence, photovoltaic, and photocurrent measurements with Rutherford backscattering

data (to determine Ti atomic densities in the films) and microwave conductivity experiments, we are able to construct a detailed picture of the optoelectronic processes in the system. A model for discussing the charge transport in the composite films is developed based on a random or biased random walk of charge through an ordered lattice of nanocrystals. We also discuss the differences in the photovoltaic mechanism between such composites and conventional, inorganic semiconductor *pn* junctions.

II. EXPERIMENT

Colloids of completely dispersed TiO_2 nanocrystals of uniform size can be prepared via a hydrolysis reaction. We obtained a well-characterized colloid (22-g TiO_2/l) of such nanocrystals in methanol (at pH 2) as a generous gift from M. Grätzel (Ecole Polytechnique Federale Lausanne). Details of the preparation of the TiO_2 colloid are found in Ref. 14. The nanocrystals are spherical in shape with 20-nm diameters and an electronic band gap of 3.2 eV, and are predominantly in anatase crystalline form (~75%). The conjugated polymer (a sulfonium precursor of PPV) was prepared as a roughly 0.7-wt % polymer in methanol,[15] and converted to the final product, PPV, by heating in vacuum (10^{-7} torr) or under flowing nitrogen at 150–200 °C. Because both components are soluble in the same solvent, there is no need to encapsulate the nanocrystals with an organic layer; composite films were obtained simply by mixing the two components in the desired weight ratio, evaporating excess solvent away to obtain a viscous solution, and spin coating onto substrates. The films are nonscattering, indicating good dispersion of the nanocrystals in the polymer matrix.

Absorption spectra were measured with a Perkin Elmer Lambda 2S Spectrometer with 2-nm spectral bandwidth. For photoluminescence efficiency measurements, mixtures were spin coated on Spectrosil substrates, and efficiencies measured using an integrating sphere technique, described previously.[16] Photoexcitation was made with the 457-nm line of an argon-ion laser, and typical excitation powers were 0.1 mW. The integrating sphere was kept under a positive pressure of nitrogen during the measurements to prevent oxygen-dependent photodegradation, and the emission collected through an optical fiber from the sphere to a calibrated photodetector.

For photovoltaic or photocurrent measurements, mixtures were spin coated on transparent conducting oxide (indium tin oxide or SnO_2:F)-glass substrates with Al contacts evaporated on top, with a portion of the ITO removed for making electrical contact to the Al (necessary to prevent short circuits through the soft polymer). Current-voltage measurements were performed in air with a Keithley 238 electrometer. Illumination was made with either white light (Xe arc lamp, ~100 mW/cm^2, AM1.5) or the 357-nm line of an argon-ion laser. For quantum yield measurements a halogen lamp-monochromator system was used, with photon fluxes of 10^{11}–10^{14} s^{-1} cm^{-2} incident at the ITO side of the composite film. The spectral bandwidth of the monochromator was 4 nm. Normalized short-circuit currents (quantum yields) as a function of excitation energy were obtained by dividing the obtained currents by the measured photon flux (using a calibrated Si diode) at each energy. Film thicknesses

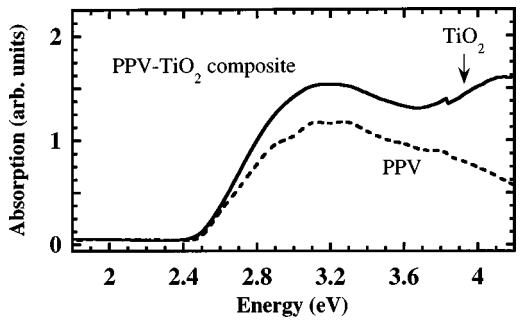

FIG. 1. Absorption spectrum of PPV alone (dashed line) and a PPV:TiO_2 composite (20-wt % TiO_2). The TiO_2 electronic band gap is at 3.2 eV, with a maximum absorption coefficient at 4.2 eV. The films are visually nonscattering.

for all samples were 100–150 nm, as measured with a Dektak instrument.

Microwave photoconductivity measurements were performed as described in detail in Ref. 17. Briefly, the experimental apparatus consists of a microwave cavity with a slit open at one end, permitting optical excitation by a Nd:YAG (yttrium aluminum garnet) laser beam (532 nm) converted to pulses of 10-ns duration and various energies by an optical parametric oscillator (photon energy 3.5 eV for band-gap excitation in the TiO_2 nanocrystals), and microwave generation and detection electronics. Excitation was done at a 3-Hz repetition rate with 2 mJ/pulse, and a beam size of about 1 cm in diameter. For microwave conductivity measurements, the films were prepared on glass and mounted in the microwave cavity at a position of maximum electric-field strength ($\sim 10^4$ V/cm). The time-dependent photoconductivity $\Delta\sigma(t)$ due to light-induced excess charge carriers in the sample is given by

$$\Delta\sigma(t) = e\Delta n(t)\mu_n + e\Delta p(t)\mu_p, \tag{1}$$

with $\Delta n(t)$ and μ_n the excess electron concentration and mobility, respectively, $\Delta p(t)$ and μ_p the corresponding properties for holes, and e the fundamental unit of charge.[18,19] The time dependence of the photoconductivity therefore mirrors the decay of the excess charge carriers. All measurements were performed in air at room temperature. For the transport model, the relevant equations were implemented in C on a computer mainframe (Digital, Inc.), and solved within minutes to several hours of real time.

III. RESULTS AND DISCUSSION

A. Optical absorption

The absorption spectrum of PPV and a 20-wt % TiO_2-PPV composite film is shown in Fig. 1. The spectrum indicates that more than 90% of the incident light is absorbed between 2.8 and 4.4 eV. The rise of the absorption due to the TiO_2 nanocrystals above band gap at about 3.2 eV is visible, and a peak occurs at 4.2 eV, the energy at which the absorption coefficient in TiO_2 is a maximum.[20] For polycrystalline TiO_2, the absorption coefficient $\alpha = 8\times10^5$ cm^{-1} at 4.2 eV indicates a dense film of thickness 16 nm for the measured film absorption of 1.3. Since the film thickness is 100 nm for this sample, the absorption implies an 16% volume fraction for the nanocrystals. A volume fraction of 17+/−1% TiO_2

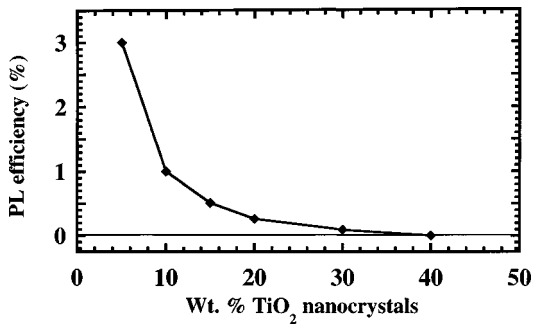

FIG. 2. Absolute photoluminescence (PL) efficiency of PPV:TiO_2 composites as a function of wt % TiO_2 nanocrystals. The PL efficiency for PPV alone was measured to be 20%.

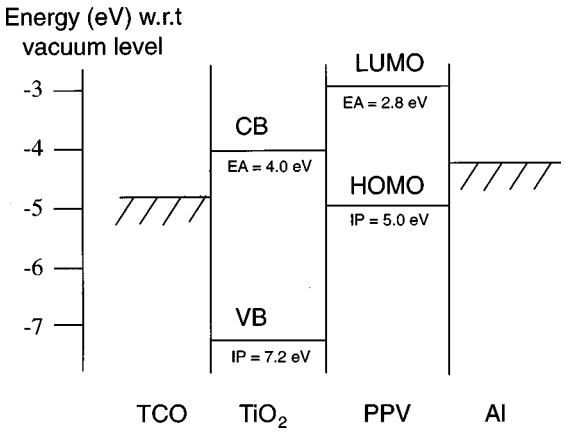

FIG. 3. Electronic energy-level diagram relative to vacuum for the TiO_2 nanocrystals (CB: conduction band; VB: valence band; EA: electron affinity; IP: ionization potential), the PPV (LUMO: lowest unoccupied molecular orbital; HOMO: highest occupied molecular orbital), and work function levels of TCO [transparent conducting oxide (ITO) or SnO_2F] and Al. The energy levels were obtained from Refs. 3 and 20.

has been independently determined for this sample by Rutherford backscattering,[21] in precise agreement with the absorption measurement. The absorption of PPV in the composites in Fig. 1 is unperturbed by the presence of the nanocrystals, displaying the same π-π^* absorption peak as for PPV alone. For higher weight fractions of TiO_2, the TiO_2 peak is correspondingly higher, and the two distinct peaks present in the spectrum of the 20-wt % composite, one due to the π-π^* absorption maximum of the polymer and the other to the band-gap onset of TiO_2, merge into a single broad absorption band dominated by the nanocrystal absorption. The absorption spectra are the sum of the absorption spectra of the two components individually, indicating that no charge-transfer bands or significant electronic interaction occurs between the materials under steady-state illumination at low intensities. The energy levels of the two components are shown in Fig. 3.

B. Photoluminescence efficiency and exciton dissociation

Composites of PPV with TiO_2 nanocrystals were studied by photoluminescence (PL) as a function of wt % of nanocrystals. For PPV alone, PL efficiencies are 0.17–0.27 depending on material quality and preparation conditions.[16] Figure 2 shows the PL efficiencies of films prepared with TiO_2 nanocrystals. Even at 5-wt % TiO_2, there is significant quenching of the polymer fluorescence (approximately 80% of the excitons are quenched as compared with PPV alone). At higher concentrations of the nanocrystal, the quenching is nearly complete. The quenching is clearly due to the presence and distribution of nanocrystals in the polymer matrix. Given an exciton diffusion length of 5–15 nm, most of the excitons must be generated within this distance of a nanocrystal and be quenched within about 1 ns, the maximum lifetime of the excitons. From optical absorption and Rutherford backscattering (RBS) measurements,[21] the volume density of TiO_2 in a 5-wt % TiO_2:PPV composite is $11+/-2\%$, or two nanocrystals per every volume cube of edge 43 nm. This volume fraction in a 5-wt % composite is slightly higher than would be expected given the densities of each component, 4 and 1.4 g/cm^3 for TiO_2 and PPV,[3,20] respectively, but at higher weight fractions the measured volume densities are in good agreement with the expected densities. The RBS measurements also indicate that the density of nanocrystals is constant across the thickness of the composite film.[21] The maximum distance of any point to a nanocrystal surface in the 5-wt % composite is about 35 nm, obtained by a straightforward geometric argument. For an ordered, close-packed lattice of spherical nanocrystals, we would have a maximum volume fraction of 52% TiO_2 based on geometric considerations. In this ideal case, each nanocrystal would be in physical contact with at least four or six others, depending on whether it is at a surface of the film or in the interior. Given that the nanocrystals will not be evenly spaced in the composites, we have no precise information about the distribution of nanocrystal spacing in the film and the degree to which the crystals are in physical contact.

The PL is quenched by a factor of approximately 7, with 5-wt % nanocrystals, which corresponds to an interfacial dissociation of more than 80% of the luminescent excitons. This result and the expected maximum distance to a nanocrystal interface of 20 nm are in reasonable accord given an exciton diffusion length of 5–15 nm and a distribution of distances from a polymer to a nanocrystal interface with a maximum of 35 nm. As the wt % of nanocrystals increases, the maximum distance to a nanocrystal interface decreases. For 40-wt % nanocrystals and a volume density of 22%, the maximum polymer-nanocrystal distance is about 18 nm, and we measure a PL efficiency of below 0.5, indicating that the luminescence is quenched by a factor of more than 20. The exciton also has a finite dimension in the polymer phase: the dimensions in a single PPV molecule have been calculated to be about 2 nm along the length of the chain and 0.4 nm transverse to it;[3] however, with more extended states in a solid film, the spatial extent of the exciton may be longer, resulting in an even smaller effective distance from polymer to nanocrystal surface. Overall, the quenching of the luminescence is nearly complete above 20-wt % TiO_2 nanocrystals, indicating that nearly all of the excitons are generated within 5–15 nm of a nanocrystal interface, that the excitons are capable of being quenched by the surface (due to charge separation, for instance), and that the nanocrystals are well mixed in the polymer.

The PL efficiency Φ depends on the fraction of absorbed photons which produce singlet excitons (the branching ratio

η), as opposed to other species such as spatially separate polaron pairs, and the probability that the singlet excitons will decay to the ground state by radiative emission, ε:

$$\Phi = \eta\varepsilon. \tag{2}$$

The values of η and ε determine the physical detail behind the luminescence efficiency observable. The measured absolute luminescence efficiency of $\Phi = 0.27$ for PPV gives a lower limit of $\eta = 0.27$, if ε is unity. As discussed in detail in the work by Greenham *et al.*,[16] the efficiency of radiative decay of singlet excitons, ε, depends on a competition between radiative and nonradiative decay rate processes, and has been estimated to be about 0.28 for PPV, implying a branching ratio η of unity (all photoexcitations produce singlet excitons). The decrease in PL efficiency in the presence of the nanocrystals indicates that either or both η and ε is reduced. The most likely interpretation is that another branching channel is added to the system, i.e., an exciton loss via charge separation which subsequently decays nonradiatively. In previous work,[13] we showed, using a microwave conductivity technique, that photogenerated excitons in PPV do indeed dissociate at a TiO_2 nanocrystal interface to give separated charges, with electrons transferred to the conduction band of the nanocrystals following polymer photoexcitation. The conduction band electrons are mobile in the microwave field and a control experiment with a film of PPV without nanocrystals displayed no such signal.

Given that the PL efficiency decrease is due to charge separation at the polymer-nanocrystal interface, a knowledge of the fraction of absorbed photons which produce excited states capable of leading to charge separation would be useful. A simple equation accounting for this is

$$\Gamma = \eta\kappa, \tag{3}$$

with Γ the fraction of charge separation events per absorbed photon (under steady-state illumination), η the fraction of absorbed photons leading to a state capable of interfacial charge separation (singlet excitons), and κ the efficiency of charge separation of the state. Thus $\Gamma + \Phi = 1$, with all absorbed photons leading to either luminescence or charge separation. In general each term in Eq. (3) is also dependent on photon energy. If we take η to be unity as discussed above (all photoexcitations produce states capable of charge separation), Γ is determined by κ via either geometric considerations (distribution of nanocrystals per unit volume, i.e., polymer-nanocrystal distance) or the probability of exciton dissociation upon reaching an interface, or both. In the case here with TiO_2 nanocrystals and nearly complete PL quenching, with all absorbed photons leading to singlet excitons which are capable of charge separation, $\kappa \cong 1$, and thus all absorbed photons lead to charge separations. In general cases of conjugated polymers mixed with nanocrystals or C_{60} molecules, the efficiency of dissociation, κ, may be lower than unity, or there may be other nonradiative channels of decay available to an exciton upon reaching the interface resulting in a less than complete PL quenching. Based on our direct observation of complete PL quenching, the microwave conductivity measurements, and taking η to be unity, we expect that all excitons are converted into separated charges in composites with 20-wt % TiO_2 and higher.

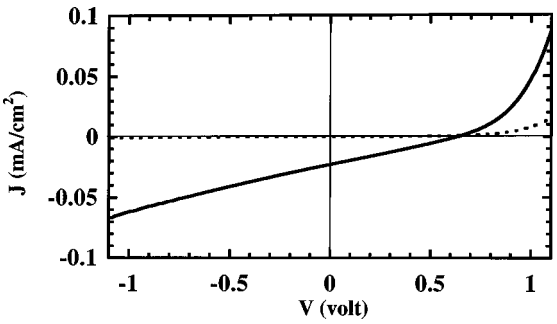

FIG. 4. Current density-voltage curve (J-V) of a typical ITO/PPV:TiO_2 composite/Al device in the dark (dashed line) and under white light illumination (100 mW/cm^2). The dark curve indicates diode behavior. The typical device size was 1–4 mm^2.

C. Photovoltaic and photocurrent properties

1. Photovoltaic properties

Photovoltaic measurements were made on the device structure Al/PPV:TiO_2 composite/ITO in the dark and under illumination, and a typical current-voltage curve is shown in Fig. 4. For a 20-wt % TiO_2 composite, the short-circuit current density in white light (100 mW/cm^2, AM1.5) is 25 μA/cm^2 with an open-circuit voltage of 0.65 V. For a 67-wt % composite, the short-circuit current increases by a factor of more than 3, to over 75 μA/cm^2, but the curve shape and open-circuit voltage remain nearly the same. The magnitude of the open-circuit voltage at a given light intensity depends on the steady-state balance between generation and recombination rate for charge separation at a polymer-nanocrystal interface with subsequent spatial separation across the film, and these are not expected to depend strongly on the density of nanocrystals in the composite. The open-circuit voltage of the device, 0.65 V, is equal to the work-function difference between Al and ITO, indicating that the spatial separation of the charges across the film is limited by the built-in electric field between the contacts. Electrons flow into the Al contact, which is consistent with the direction of the built-in electric field (Al with a lower work function than ITO, see Fig. 3). In reverse bias, the photocurrent under the white light illumination increases by a factor of 2 at -2.0 V for a given composite, but remains at this level at larger reverse bias voltages. The effect of the bias indicates an improvement in an efficiency of collecting separated charges in the device rather than an improvement in the efficiency of charge separation efficiency, since we observe from the photoluminescence measurements that nearly all excitons have been converted to separated charges under zero bias.

2. Photocurrent quantum yields

Quantum yields (electrons/incident photons) are 1–2 % between 2.5 and 3 eV, and over 10% above 3.2 eV at short circuit for a 20-wt % TiO_2 composite. These values are increased by a factor of 2–3 for a 67-wt % TiO_2. The spectral response of the photocurrent at short circuit for a composite is shown in Figs. 5 and 6. The photocurrent onset is at 2.35 eV, consistent with that for Al/PPV/ITO structures (without nanocrystals).[22] However, the current density is two orders of magnitude higher than that found in PPV-only structures, due to an improved efficiency in exciton dissociation in the

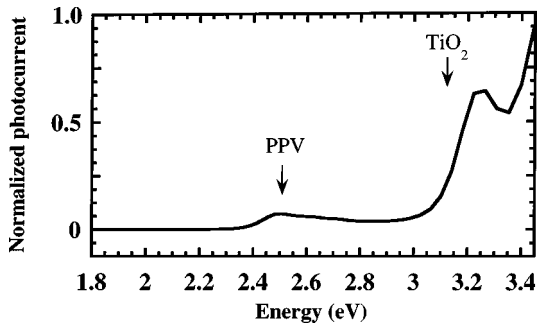

FIG. 5. Spectral response for an ITO/PPV:TiO_2 composite/Al device. Quantum yields (collected electrons/incident photons) are in the range of 2–3 % over the spectral region 2.3–2.7 eV for a 67-wt % TiO_2:PPV composite; quantum yields above 3.3 eV are over 10%. The spectral bandwidth was 4 nm with photon fluxes of $10^{11}-10^{14}\,s^{-1}\,cm^{-2}$.

presence of the nanocrystals. At photon energies above 3.2 eV, the photocurrent quantum yield increases rapidly to nearly 15% at 3.4 eV. The magnitude of the short-circuit current is linear with monochromatic light intensity (argon-ion laser, 357-nm line) in the range of $10^{11}-10^{14}$ photons $cm^{-2}\,s^{-1}$, the same range of incident light intensity in which the quantum yields were measured; this indicates that the measured quantum yields are not a function of the light intensity used in the measurement. The quantum yield at short circuit as a function of photon energy, $Q(E)$, can be accounted for by the product of three factors: the fraction of photons absorbed, A; the charge separation yield per absorbed photon, κ; and the charge transport efficiency or probability of collecting the charge at a contact, φ. The factor φ will depend on the competition between charge transport time to a collecting contact and recombination. Of these factors, only the fraction of absorbed photons and collection efficiency depend on the photon energy:

$$Q(E)=A(E)\kappa\varphi(E) \tag{4}$$

because the photoluminescence work (PL quenching by the same factor at all energies) suggests that, in a heterogeneous mixture of two components with different electrochemical potentials, the charge separation efficiency κ is not determined by the energy of the excitation, but rather only by the energetic and electrical characteristics of the interface. The collection efficiency φ may depend on excitation energy, since different excitations may lead to charge-separated

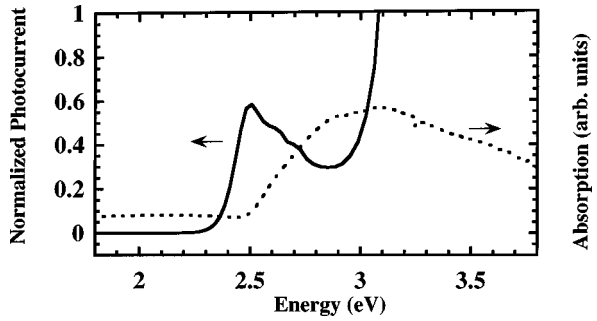

FIG. 6. Spectral response for an ITO/PPV:TiO_2 composite/Al device compared with PPV-only absorption. The spectral bandwidth was 4 nm with photon fluxes of $10^{11}-10^{14}\,s^{-1}\,cm^{-2}$.

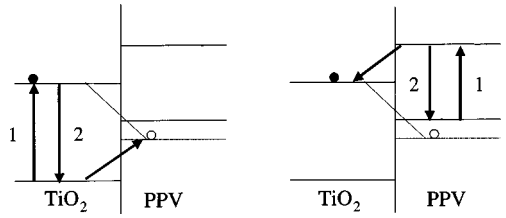

FIG. 7. Schematic diagram of the various excitation, charge transfer, and decay pathways available in a conjugated polymer-nanocrystal composite. The filled circles indicate electrons, and the open circles represent holes. Process 1 indicates photoexcitation; process 2 indicates decay of the electronic excited state; the dark slanting lines with arrows indicate a hole or electron transfer process (left and right sides, respectively); and the thin lines connecting the conduction band of TiO_2 with the hole level in PPV indicate an interfacial recombination process. The state levels are depicted as in Fig. 3, with the holes placed at slightly lower energy than the polymer LUMO (lowest unoccupied molecular orbital).

states with different lifetimes and thus be collected with different efficiencies. We examine this possibility in Sec. III C 3.

3. Electron vs hole transfer across the conjugated polymer-TiO_2 interface

The increase in the quantum yield at photon energies higher than 3.2 eV in our devices cannot be attributed solely to the absorption of the PPV, since the absorbance of PPV increases only by a factor of 2 from 2.6 to 3.2 eV, for example, while the response increases by a factor of 8. In PPV-only devices the quantum yield declines to zero in this spectral region.[22] The increase instead must be due to absorption directly into the TiO_2 nanocrystals, producing free charge carriers above the band gap. Since the absorbance of the nanocrystals in our composites is not significantly higher than that of the PPV, the main factor responsible for the increase in quantum yield must be accounted for by $\varphi(E)$, the probability of collecting the charge at a contact. Figure 7 illustrates the possible excitation, charge transfer, and decay pathways involved in the composite. Process 1 represents photoexcitation in the polymer and nanocrystal phases; process 2 represents the internal decay of the excitation energy via radiative and nonradiative pathways; the dark arrows slanting left and right represent hole and electron transfer across the interface, respectively; and the slanting thin lines represent recombination across the interface between the spatially separated electrons and holes. The levels of the holes are placed slightly lower in the schematic than the lowest unoccupied molecular orbital level of the PPV, since they are presumed to somewhat polarize the surrounding polymer.

The time scales for the internal decay of the excitation following photoexcitation of either PPV or TiO_2 are known. Process 2 in PPV alone, the exciton decay, typically occurs within 1–2 ns (radiative and nonradiative decay), measured from photoluminescence and photoexcitation spectroscopy.[3,23] We measured process 2 in TiO_2 nanocrystals, the recombination of free charge carriers, by a time-resolved microwave photoconductivity technique. Figure 8 shows the microwave photoconductivity trace measured when the TiO_2

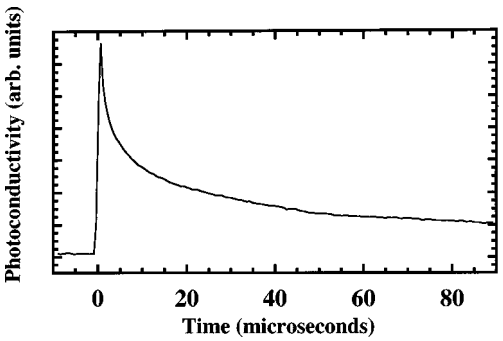

FIG. 8. Microwave photoconductivity of TiO_2 nanocrystals in air following a 10-ns flash of 2-mJ light (3.5 eV). References 13 and 17 contain details of the experimental setup.

nanocrystals in air are excited above the band gap at 3.5 eV. Figure 8 indicates that half of the free charge carriers recombine in about 10 μs and 80% in 90 μs. The decay of the free charge carriers is not expected to be significantly altered in TiO_2:PPV composites.

The recombination reaction between the spatially separated electrons and holes in the composite has also been measured by the same technique.[13] The process occurs in hundreds of nanoseconds to several microseconds and, although measured only for polymer photoexcitation, is expected to be the same for either polymer or nanocrystal excitation since the resulting state (electrons in nanocrystals and holes in polymer) is the same. The time scales for the electron and hole transfer processes have not been measured. If we attribute the increase in the photocurrent quantum yield above 3.1 eV of the composite devices to a longer-lived charge-separated state, this implies that either the hole transfer process from TiO_2 to PPV is slower than the electron transfer process from excitons in PPV, or that some process preceding hole transfer is slower. In either case, it takes longer to reach the charge-separated state and thus longer for charge recombination. With τ the total time required for relaxation of the excitation energy:

$$\tau = \sum k_{\mathrm{ct}}^{-1} + k_0^{-1} + k_r^{-1}, \tag{5}$$

and k_{ct} and k_r the charge-transfer and recombination rate constants, respectively, and k_0 the rate constant for some process which precedes charge transfer, we expect that k_0^{-1} or k_{ct}^{-1} or both are longer following TiO_2 excitation than the corresponding processes following polymer excitation. The fact that free-charge-carrier decay in TiO_2 nanocrystals alone (Fig. 8) decays much more slowly than the (interfacial) recombination process in composites suggests that a longer length of time could elapse before hole transfer to the polymer occurs. If the longer time to reach the charge-separated state is due to the hole transfer process itself, this might be accounted for by a larger effective mass of the holes than the electrons, but a detailed analysis of this is beyond the scope of the present paper.

D. Spatial origin of the photocurrent

We now consider the important question of where in the composite film the observed photocurrent in the Al/PPV:TiO_2 composite/ITO device originates. For both PPV and TiO_2 photoexcitation, the net result is the same: a light-induced excess of electrons is in the conduction band of the nanocrystals, and corresponding holes in PPV. The efficiency of collecting charge at a contact will depend on the site of charge separation in the film, since different locations are at different distances from the contact. The polymer phase is continuous throughout the composite, but only some fraction of the nanocrystals is in physical contact with other nanocrystals. Therefore, a path exists from any charge separation site in the composite for hole transport to the ITO contact, but there may not be such a path for the electrons in the TiO_2 to the Al contact. Furthermore, even if conducting pathways do exist for the electrons in the TiO_2, they may not be transported efficiently through the network due to energetic barriers or grain boundaries between nanocrystals. Thus we expect that the magnitude of the short-circuit currents will be limited by electron transport through the nanocrystalline phase rather than by hole transport through the polymer phase. We also assume that charge transfers or recombination at the contacts of the device are not limiting factors in the quantum yields.

We observe a 2–3 increase in the short-circuit quantum yields of our devices going from 20- to 67-wt % TiO_2. Since the PL measurement indicates that over 95% of the excitons are quenched (via charge separation) in the 20-wt % TiO_2 composite, it is possible that the increase is simply due to an increase in absorption at higher TiO_2 contents (with quantum yields of charge collection significantly higher for nanocrystal excitation than for polymer excitation). Another possibility is that significantly more electrons in the film are able to reach the collecting contact, since there are more continuous paths from any charge separation site to a contact available at higher weight fractions of nanocrystals. However, we can account for the *absolute* quantum yields in any of our composites by only considering the charge separation events in the first nanocrystal layer from the Al contact. With the measured absorbance of each component in film and the expected charge generation profile $I_f = I_0 e^{-A}$, with I_0 the incident light intensity at the ITO contact, I_f the light intensity at the Al contact, and A the film absorbance, we can estimate an upper limit for the photocurrent quantum yield of charge collected from just a single TiO_2 nanocrystal layer at the Al contact. For a single pass of light, neglecting reflection from the Al contact—which will raise the estimate—and assuming that every photon absorbed leads to a charge separation event, we calculate a maximum quantum yield of about 40% for a 67-wt % TiO_2-PPV composite at the first layer of nanocrystals at the Al contact, assuming that all excitons within 15 nm of the electrode are converted to collected charges and the measured total film absorbance $A \cong 1.0$ for a 100-nm-thick film. Since our measured quantum yields of 10–15 % for TiO_2 excitation (and 1–2 % for PPV excitation) are well below this, we have no assurance that the charge is collected from nanocrystals throughout the film rather than only at the interface. Our argument does not rule out charge transport between nanocrystals, it only demonstrates that the existence of a photocurrent in device structures based on conjugated polymer-nanocrystal composites does not necessarily indicate that charge transport occurs between the nanocrystals. We will consider the transport issue more

quantitatively in following sections. In related work with a PPV derivative mixed with a CdSe nanocrystal,[9] the authors found a more than tenfold increase in short-circuit quantum yield going from 40- to 90-wt % nanocrystals, and concluded from this that the significant increase in photocurrent at 90 wt % is largely due to a percolation effect in the TiO_2 phase, i.e., that the threshold for percolation is reached where there is a high probability of finding a continuous pathways from most sites in the lattice to the collecting contact. However, the tenfold increase might also be accounted for by a combination of a decrease in PL efficiency (increase in charge separation efficiency of excitons) with a higher absorption of the film (increase in excitons), leading to an increase in the photocurrent.

E. Charge-carrier recombination and transport time scales

1. Carrier recombination

Apart from the question of whether electrons are collected from throughout the TiO_2 nanocrystal film or from only a single interfacial layer near the contact, carrier transport in both TiO_2 and PPV phases must compete with recombination. We will use the photocurrent quantum yield to estimate the time scale of charge transport in the 67-wt % TiO_2:PPV composite as follows. First, we assume that all incident photons are absorbed in the composite. This is a reasonable assumption since, from the measured absorbance, less than 10% of the incident light reaches the Al back contact. Second, we assume that all absorbed photons are converted into separated charges based on our arguments from above. Using Eq. (4) we are left with the factor φ, the probability of charge collection at a contact: the quantum yield Q is determined by the charge transport and recombination rate processes, not by absorption or charge separation efficiency. The probability of charge collection φ is determined by the mean time required for a carrier to be collected at a contact, τ,

$$\varphi = R(\tau)/R(0), \tag{6}$$

with $R(\tau)$ given by the measured recombination process, and $R(0)$ for normalization. An overall quantum yield Q of 1–2 % implies a φ of 1–2 % and a 98–99% probability of recombination. Recombination of the separated charges occurs in a complex manner with half of the initial signal amplitude, decaying in 600 ns in a nonexponential fashion.[13] The part of the decay after 800 ns can be well fitted to a sum of two exponentials with time constants of 4.3 and 80 μs and relative amplitudes of 0.7 and 0.3, respectively. From these data, we infer that the mean time for charge transport in the films is 200–300 μs. As discussed above, we attribute the much higher quantum yield (10–15 %) above 3.2 eV to TiO_2 nanocrystal excitation with hole transfer to the PPV or some preceding process as the limiting step, not the recombination process, which leads to a longer-lived charge-separated state.

2. Carrier transport from experimental measurements and in a lattice model

First we consider the dark carrier densities and mobilities in both phases. In PPV, a *p*-doped material, the intrinsic hole concentration is estimated to be $p = 10^{14}\,\mathrm{cm}^{-3}$, and the intrinsic electron concentration, n to be two orders of magnitude lower than this.[3] TiO_2, as prepared and used in our composites, is expected to be n doped due to adventitious O_2 doping, with an estimated doping density of about $10^{17}\,\mathrm{cm}^{-3}$.[24,25] Under white light (100 mW/cm^2, AM1.5), we can expect a maximum steady-state photoinduced excess charge density for either carrier $(\Delta n, \Delta p)$ of $10^{17}\,\mathrm{cm}^{-3}$ with $\Delta n = \Delta p$.[26] With interfacial charge separation with electrons to the nanocrystals and holes to the polymer, $\Delta n \cong n$ is the same order of magnitude or less than the dark density; but $\Delta p \ll p$ is several orders of magnitude lower than the dark density. This indicates that a hole photodoping effect will potentially be operating in the polymer phase under these illumination levels, and may contribute to an improvement in photocurrent as the illumination intensity is increased. Charge carriers in both phases are therefore majority carriers, with the predominant recombination loss occurring at the interface between the components. Photocurrents are due to the collection of each carrier at opposite electrodes. Electron mobilities for bulk TiO_2 are $\mu_{n,\mathrm{TiO_2}} = 0.1\text{–}1\,\mathrm{cm}^2\,\mathrm{V}^{-1}\,\mathrm{s}^{-1}$, and for holes at least an order of magnitude lower,[20] but it is not known how much these values are reduced in a film of nanocrystals with grain boundaries between the crystals. Assuming a mobility then of $\mu_{n,\mathrm{TiO_2}} = 0.1\,\mathrm{cm}^2\,\mathrm{V}^{-1}\,\mathrm{s}^{-1}$, we obtain a diffusion constant $D = 2.5\times10^{-5}\,\mathrm{cm}^2\,\mathrm{s}^{-1}$ for the conduction-band electrons in bulk. For PPV, the hole mobility is $\mu_{p,\mathrm{PPV}} \leqslant 10^{-4}\,\mathrm{cm}^2\,\mathrm{V}^{-1}\,\mathrm{s}^{-1}$ (Ref. 3), and electron mobilities several orders of magnitude smaller. For PPV then, the diffusion constant of holes is $D = 2.5\times10^{-6}\,\mathrm{cm}^2\,\mathrm{s}^{-1}$ at 300 K by Einstein's relation.

Now we model the transport and charge collection probability, and compare this with the measured values. For simplicity, we will assume our composites are composed of a well-ordered square TiO_2 nanocrystal lattice with PPV in the interstitial space. A real system with disordered nanocrystals will exhibit less efficient charge transport through the network, so the ideal system represents an upper limit in performance. We consider only the electrons moving in the nanocrystal phase, although a similar argument can be made for the holes in the polymer phase. We assume that all electrons in the conduction band of the first layer of nanocrystals at the Al contact are collected with unity probability, but this does not change the conclusions of the argument. The remaining electrons must random walk through the lattice to be collected at the contact. Taking a hopping model for the transport, we have in principle six different probabilities per unit time (rate constants) for hopping $\{p_1,\ldots,p_6\}$, depending on the direction of the hop: p_1 toward the collecting contact, p_2 away from it, and $p_3,\ldots,p_6$ in a sideways fashion within a lattice layer. The difference in the hop probabilities arises from the built-in electric field oriented toward the collecting contact. To estimate the relative magnitudes of the hop probabilities, we compare the diffusion and drift velocities of the electrons. For the thermal velocity we have the formula $m_e v_{\mathrm{th}}^2 = 3/2\,\mathrm{kT}$, with m_e the effective mass of the electron, v_{th} the thermal velocity, k Boltzmann's constant, and T the temperature. Taking m_e to be 100 times that of a free-electron mass,[17] we have $v_{\mathrm{th}} = 1.1\times10^4$ cm/s at 300 K. We calculate the drift velocity from the formula $v_d = \mu E$, with v_d the drift velocity, μ the electron mobility in the TiO_2 conduction band, and E the built-in electric field. Taking μ

$=0.1\,\mathrm{cm^2\,V^{-1}\,s^{-1}}$ and $E=5\times10^4$ V/cm (from 0.7 V across 150 nm) gives $v_d=4\times10^3$ cm/s. Since our estimate of the mobility assumes bulk and is probably too high given grain boundaries between nanocrystals, we expect that the drift velocity is much smaller than the thermal velocity. We conclude, therefore, that the main force behind carrier transport is thermal diffusion, biased slightly by the built-in electric field.

Following this argument, we estimate the maximum distance an electron will travel in bulk TiO_2 using the diffusion constant of the conduction band electrons ($D=2.5\times10^{-5}\,\mathrm{cm^2\,s^{-1}}$). The electrons in bulk TiO_2 will diffuse according to the formula $L^2/D=\tau$, with L the average distance traveled in time τ. Taking $\tau=100\,\mu$s as the upper limit allowed for transport by the recombination process (cf. above), we determine $L\cong500$ nm. We now picture that distance as a series of hops between individual sites (nanocrystals) of diameter 25 nm, and find an upper limit for the number of hops before recombination: 20. The estimate implies an upper limit for the time to hop between nanocrystals of $T\cong10\,\mu$s. However, in a network of TiO_2 nanocrystals, the diffusion constant is expected to be significantly lower than the bulk value. From recombination measurements in a network of dye-sensitized TiO_2 nanocrystals[17] and the known quantum yields, we estimate a diffusion constant of order $10^{-7}\,\mathrm{cm^2\,s^{-1}}$; using this and following the same argument as above gives an average hop time of about 100 μs between nanocrystals. For a PPV:TiO_2 composite system, with charge recombination complete in 100 μs, we can therefore expect charge collection only from the first nanocrystal layer at the electrode interface.

3. Carrier transport: A general case of a conjugated polymer:nanocrystal composite

We now examine the general case of a conjugated polymer:semiconductor nanocrystal composite in which excitons are dissociated at the interface between the components, with electrons transferred to the nanocrystal conduction band. We will assume that the photocurrent is limited by the collection of the electrons rather than holes in the polymer phase. We would like to know the probability that an electron introduced at some site s in the film can reach the collecting contact subject to charge recombination, as a function of diffusion constant and position within the nanocrystal network. We will again take a close-packed, ordered square lattice of nanocrystals as our model system, and assume that the electrons migrate mainly according to diffusion with a negligible drift bias. An electron in the bulk will have six hop possibilities and associated probabilities $\{p_1,\ldots,p_6\}$, with $\Sigma p_i=1$. We define the nanocrystal layer at the electrode interface as layer 1, and take $\{k_1,\ldots,k_6\}$ as the number of occurrences of each hop direction in a given path sequence of N steps. The probability P for a charge not reaching the first layer from others layers $\{2,\ldots,n=L\}$ in the lattice is then given by

$$P=\sum_{k_1,\ldots,k_6} N!/(k_1!k_2!k_3!k_4!k_5!k_6!)p_1^{k1}p_2^{k2}p_3^{k3}p_4^{k4}p_5^{k5}p_6^{k6}, \tag{7}$$

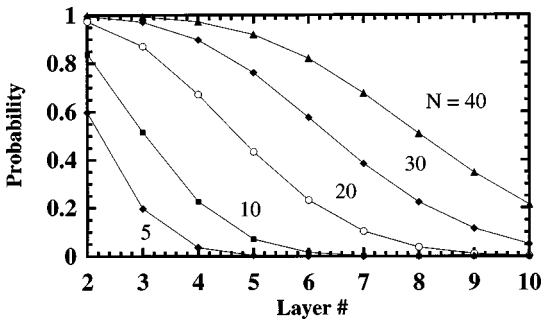

FIG. 9. Results of a random walk of charge of N steps in a close-packed, well-ordered lattice (of nanocrystals): the probability to reach the first nanocrystal layer (at the interface with the electrode) starting from the second to the tenth layers. Details of the model and the implications of the results are discussed in the text.

with a sum over all with the possible sequences in a path of length N, with the obvious condition that $\Sigma k_i=N$ and the boundary condition $k_i<L-1$ with L the layer number. The boundary condition limits the sum to only those path sequences which do not allow the charge to reach the first layer. We take the probability for hopping in any of the six directions to be equal ($p_1=p_2=p_3=p_4=p_5=p_6=\frac{1}{6}$), although a biased random walk can be obtained directly by including other values for the hop probabilities. Equation (7) therefore becomes

$$P=\tfrac{1}{6}{}^N\sum N!/(k_1!k_2!k_3!k_4!k_5!k_6!). \tag{8}$$

The results of a random walk of length N in the nanocrystal lattice are shown in Fig. 9, plotted as the probability to reach the first layer from a given layer (2,...,10). For walks of five steps, there is only a 60% probability of a charge from the second layer reaching the first layer, and a 20% probability to reach it from the third layer. For walks of 20 steps or more, there is a better than 50% probability of the electrons reaching the first layer from within the fourth layer. If we assume the probability of collecting an electron from the first layer is unity, these results can be used directly to determine the spatial origin of the collected charge since $n(L)=P(L)G(L)$, where $P(L)$ is the probability for collecting an electron at the contact from layer L in the lattice, and $G(L)$ is the number of charges photogenerated within layer L (directly determined from the absorption profile). Again, these results are for an ordered, close packed lattice; in the real situation, the probabilities shown in Fig. 9 will be smaller.

For a general case with τ given by the recombination time (we take this to be the time for 90% of charges to recombine) and using the diffusion formula, $Nd\cong(\tau D)^{0.5}$, with d the hop distance (i.e., nanocrystal diameter). To collect most of the electrons from the within the first five or six layers in the ideal lattice, would require a minimum of $N=40$. For nanocrystals of 25-nm diameter ($d=25$) and an upper limit for the diffusion constant through the network, $D=2.5\times10^{-5}\,\mathrm{cm^2\,s^{-1}}$, this corresponds to a recombination time τ of 400 μs. Now consider a well-ordered lattice of nanocrystals with grain boundaries and a lower diffusion constant, order of $10^{-7}\,\mathrm{cm^2\,s^{-1}}$, as discussed above. To collect charge from the first five or six layers via the random walk, we

would need a minimum again of 40 steps, and this implies a demand of $\tau = 0.1$ s for the recombination time. Since most of the separated charges in PPV:TiO_2 nanocrystal devices recombine within hundred of nanoseconds to microseconds (cf. above, Sec. III E 1), only charge generated within one layer in the lattice from the contact will have an appreciable probability of being collected.

4. Comparison of semiconductor nanocrystal:conjugated polymer photovoltaic devices with silicon pn junctions

It is worthwhile to compare the mechanisms by which conventional, silicon *pn*-junction photovoltaic devices work with those based on conjugated polymer composites (nanocrystals, C_{60}, etc.). The key differences are that (1) silicon has a much higher charge mobility than either conjugated polymers or nanocrystals, typically on the order of 10 or 100 $cm^2\,V^{-1}\,s^{-1}$ depending on the silicon morphology and doping density;[26,27] and (2) the device is a bilayer, junction device. The higher mobility means that the overall charge-carrier motion is strongly influenced by the built-in electric field (drift velocities are comparable to thermal velocities). By contrast, in conjugated polymer:nanocrystal devices, carrier mobilities are at least two or three orders of magnitude lower, so charge motion is mainly diffusive and thus less efficient. The second difference, the single junction between the *n*- and *p*-type layers, means that once the carriers have been separated across the interface region, they encounter only a minority of oppositely charged carriers in their transit to collecting contacts. In the composite devices, however, the charge is able to recombine across the interface between the separate phases throughout its transit to an electrode contact. In other words, the interfacial area, the region expected to produce the most carrier recombination due to surface states, is distributed over the entire device. The third main difference between the two types of devices is that even allowing for the major loss of efficiency due to the first two factors, a composite device must also provide continuous paths in each phase to the collecting contacts, and there is no guarantee that such paths will exist in composites or that efficient transport will occur between the discrete components of nanocrystals or C_{60} molecules.

It appears, based on these very substantial differences, that these composite photovoltaic devices may never reach the collection efficiencies of conventional *pn* junctions (typically over 70%). However, recent demonstrations of efficient molecular systems, such as that introduced by Regan and Grätzel based on dye-sensitized TiO_2 nanocrystals in an electrolyte, demonstrate otherwise.[28] The device has a 60% quantum yield at the maximum and produces over 10 mA/cm^2 under white-light conditions (100 mW/cm^2). In this device, as in the conjugated polymer:nanocrystal device presented here, the charge motion is mainly diffusive. However, the crucial factor which underlies the efficiency of the dye-sensitized system is that the recombination time is quite long, ranging from hundreds of milliseconds to seconds.[17] Since the device is a photoelectrochemical cell, the recombination is not between holes and electrons directly but rather between electrons and an ionic, electron acceptor in solution which may be advantageous from the point of view of reducing the recombination rate. However, it is reasonable to expect that through control of the interfacial area and morphology of nanocrystal:conjugated polymer composites, comparable efficiencies are possible.

IV. CONCLUSIONS

We have introduced photovoltaic devices of a composite of TiO_2 nanocrystals and a conjugated polymer, PPV. We have also analyzed in detail the mechanisms underlying the device, including exciton dissociation, charge recombination, and transport, paying particular attention to the composite morphology and energy levels of the electronic states in both components. Photogenerated excitons in the polymer or band-gap absorption in the nanocrystals lead to charge separation at the interface between the components (electrons to the nanocrystals and holes to the polymer, respectively), and in a device structure some of the photogenerated charge carriers are collected at the electrodes. With nearly complete photoluminescence quenching at concentrations of 20-wt % TiO_2 nanocrystals and higher, we have all absorbed photons leading to charge separation. We conclude therefore that the quantum yields of collecting charge in the device are limited by the charge transport and recombination rate processes, not by absorption or charge separation efficiency. The quantum yields of the device are significantly higher ($>10\%$) above 3.2 eV than between 2.5 and 3 eV, and we attribute this to band-gap absorption in the nanocrystals, producing free carriers which require a longer time to recombine than for the corresponding process following excitation in the polymer. We argue that the existence of a photocurrent from the device does not guarantee that charge transport occurs through a network of the nanocrystals, since the absolute quantum yields may be accounted for by charge transfer from a single nanocrystal layer at the interfacial contact; in general, in conjugated polymer composites with nanocrystals (or some other charge acceptor, such as C_{60}) more direct evidence is required to prove that photocurrents are actually due to charge percolating through a network of the nanocrystals. By using a random-walk model of electrons diffusing through a close-packed, ordered, lattice of nanocrystals we determine the requirements for efficient collection of charge as a function of distance from the electrode, recombination time, and diffusion constant in the network. The model suggests that even given an ordered lattice and a reasonably long recombination time, most of the collected charge in the TiO_2-PPV devices will originate from charge separation events within the first one or two nanocrystal layers at the electrode.

ACKNOWLEDGMENTS

This work was supported by E.U. Contract No. JORCT960107. The author gratefully acknowledges R. H. Friend and N. C. Greenham of the Cavendish Laboratory, Cambridge, U.K. and St. John's College, Cambridge, for hosting a stay to complete the photoluminescence experiments, and R. E. I. Schropp of Universiteit Utrecht, The Netherlands, for providing an environment in which the rest of the work was made possible.

[1] A. P. Alivisatos, Science **271**, 933 (1996).
[2] D. L. Klein, R. Roth, A. K. L. Lim, A. P. Alivisatos, and P. L. McEuen, Nature (London) **389**, 699 (1997).
[3] N. C. Greenham and R. H. Friend, in *Solid State Physics*, edited by H. Ehrenreich and F. Spaepen (Academic, San Diego, 1995), Vol. 49, p. 1.
[4] J. J. M. Halls, K. Pichler, R. H. Friend, S. C. Moratti, and A. B. Holmes, Appl. Phys. Lett. **68**, 3120 (1996).
[5] K. E. Ziemelis, A. T. Hussain, D. D. C. Bradley, R. H. Friend, J. Rühe, and G. Wegner, Phys. Rev. Lett. **66**, 2231 (1991).
[6] P. J. Hamer, K. Pichler, M. G. Harrison, R. H. Friend, B. Ratier, A. Moliton, S. C. Moratti, and A. B. Holmes, Philos. Mag. B **73**, 367 (1996).
[7] P. Dyreklev, O. Inganäs, J. Paloheimo, and H. Stubb, J. Appl. Phys. **71**, 2816 (1992).
[8] Y. Wang and N. Herron, Chem. Phys. Lett. **200**, 71 (1992).
[9] N. C. Greenham, X. Peng, and A. P. Alivisatos, Phys. Rev. B **54**, 17 628 (1996).
[10] J. J. M. Halls, C. A. Walsh, N. C. Greenham, E. A. Marseglia, R. H. Friend, S. C. Moratti, and A. B. Holmes, Nature (London) **376**, 498 (1995).
[11] G. Yu, J. Gao, J. C. Hummelen, F. Wudl, and A. J. Heeger, Science **270**, 1789 (1995).
[12] K. Yoshino, X. H. Yin, K. Muro, S. Kiyomatsu, S. Morita, A. A. Zakhidov, T. Noguchi, and T. Ohnishi, Jpn. J. Appl. Phys. **32**, L357 (1993).
[13] J. S. Salafsky, W. H. Lubberhuizen, and R. E. I. Schropp, Chem. Phys. Lett. **290**, 297 (1998).
[14] M. Nazeeruddin *et al.*, Helv. Chim Acta **73**, 1788 (1990).
[15] P. L. Burn, D. D. C. Bradley, R. H. Friend, D. A. Halliday, A. B. Holmes, R. W. Jackson, and A. Kraft, J. Chem. Soc., Perkin Trans. 1 **1**, 3225 (1992).
[16] N. C. Greenham, I. D. W. Samuel, G. R. Hayes, R. T. Phillips, Y. A. R. R. Kessener, S. C. Moratti, A. B. Holmes, and R. H. Friend, Chem. Phys. Lett. **241**, 89 (1995).
[17] J. S. Salafsky, W. H. Lubberhuizen, E. van Faassen, and R. E. I. Schropp, J. Phys. Chem. B **102**, 766 (1998).
[18] M. Kunst and G. J. Beck, Appl. Phys. **60**, 3558 (1986).
[19] R. Fessenden and P. Kamat, Chem. Phys. Lett. **123**, 233 (1986).
[20] H. O. Finklea, in *Semiconductor Electrodes*, edited by H. O. Finklea (Elsevier, New York, 1988), Chap. 1.
[21] J. S. Salafsky, H. Kerp, R. E. I. Schropp, Synth. Met. (to be published).
[22] R. N. Marks, J. J. M. Halls, D. D. C. Bradley, R. H. Friend, and A. B. Holmes, J. Phys.: Condens. Matter **6**, 1379 (1994).
[23] M. Yan, L. J. Rothberg, F. Papadimitrakopolous, M. E. Galvin, and T. M. Miller, Phys. Rev. Lett. **72**, 1104 (1993).
[24] R. H. Wilson, L. A. Harris, and M. E. Gerstner, J. Electrochem. Soc. **114**, 172 (1979).
[25] G. Rothenberger, D. Fitzmaurice, and M. Grätzel, J. Phys. Chem. **96**, 5983 (1992).
[26] M. A. Green, *Solar Cells*, Prentice-Hall Series in Solid State Physical Electronics, Vol. XIV (Prentice-Hall, Englewood Cliffs, NJ, 1982).
[27] S. M. Sze, *Semiconductor Devices* (Wiley, New York, 1985).
[28] B. O'Regan and M. Grätzel, Nature (London) **353**, 737 (1991).